Industrial Crops & Products 154 (2020) 112688

Contents lists available at ScienceDirect

Industrial Crops & Products

journal homepage: www.elsevier.com/locate/indcrop

Cannabidiol-enriched hemp essential oil obtained by an optimized microwave-assisted extraction using a central composite design

Dennis Fiorini[a], Serena Scortichini[a], Giulia Bonacucina[b], Nicolas G. Greco[b], Eugenia Mazzara[b], Riccardo Petrelli[b], Jacopo Torresi[b], Filippo Maggi[b,*], Marco Cespi[b]

[a] School of Science and Technology, University of Camerino, 62032 Camerino, Italy
[b] School of Pharmacy, University of Camerino, 62032 Camerino, Italy

ARTICLE INFO

Keywords:
Hemp
Essential oil
Cannabidiol
Microwave-assisted extraction
Hydrodistillation
Design of an experiment

ABSTRACT

The increase of cultivation of industrial hemp (*Cannabis sativa* L.) all over the world offers new opportunities for the industry to manufacture innovative products from this multipurpose crop. In this regard, the hemp essential oil represents a niche product with potential interest for the pharmaceutical, nutraceutical, cosmeceutical and agrochemical companies. On this basis, in the present work we used the microwave-assisted extraction (MAE) to get an essential oil enriched in bioactive compounds, especially cannabidiol (CBD), from the dry inflorescences of the Italian variety CS (Carmagnola Selezionata). For this purpose, the operative conditions to increase the essential oil yield and CBD concentration in terms of microwave irradiation power (W/g), extraction time (min) and water added to the plant matrix after moistening (%), were optimized using a central composite design (CCD) approach using a Milestone ETHOS X device. The conventional hydrodistillation (HD) performed for 240 min was used for comparative purposes. The qualitative compositions of essential oils obtained by MAE and HD were analysed by GC-MS, whereas the quantitative detection of CBD and main terpenoids (α-pinene, β-pinene, myrcene, limonene, terpinolene, (*E*)-caryophyllene, α-humulene and caryophyllene oxide) was achieved by GC-FID. Furthermore, the enantiomeric distribution of the chiral constituents (α-pinene, β-pinene, limonene, (*E*)-caryophyllene and caryophyllene oxide) was determined using chiral chromatography. Results showed that the MAE treatment, using high irradiation power and relatively long extraction times, increased significantly the content of CBD in the essential oil while maintaining high oil yield values when compared with conventional HD. The enantiomeric excess of three chiral monoterpenes (α-pinene, β-pinene and limonene) was determined, with the (+)-enantiomers being predominant, whereas (*E*)-caryophyllene and caryophyllene oxide were enantiomerically pure. In conclusion, the MAE was successfully applied to hemp dry inflorescences in order to obtain a CBD-rich essential oil which may be exploited in several industrial applications.

1. Introduction

Hemp (*Cannabis sativa* L.), also known as the 'fibre-type' cannabis, is a legal crop cultivated from ages all around the world and its different parts, e.g. fibre, seeds, leaves and flowers are exploited in several sectors such as automotive industry, construction, paper, innovative materials, bioenergy, textile, varnishes and inks, as well as in medicine, foods, nutraceuticals and cosmetics (Ranalli and Venturi, 2004).

Hemp is an eco-friendly and sustainable crop since it enriches the soil in organic matter (> 10 t/ha), requires no agrochemical input and moderate fertilizer requirement, and owns adsorption properties toward pesticides, that is helpful in sustainable agricultural systems (Amaducci et al., 2008; Finnan and Styles, 2013; Vukčević et al., 2015). Indeed, hemp can be used in crop rotation with wheat, barley, corn and sunflower (Finnan and Styles, 2013). Different varieties are cultivated in the EU (EC Regulation, 2004), with most of them coming from France and Italy (Cappelletto et al., 2001). At present, the EU is the third producer of hemp in the world after China and Canada, with 25,000 ha of cultivations (Di Candilo, 2006). In Italy the hemp cultivation area is estimated at around 4000 ha with about 2000 farmers, most of them using organic agriculture (EC Regulation, 2007), and an overall income of ~ 40 mln € per year.

Nowadays, *C. sativa* provides the bulk material for medical preparations, namely Bedrocan®, Epidiolex®, Sativex®, and others, that are used for the treatment of chronic diseases, multiple sclerosis, neuropathic pain and epilepsy (Barnes, 2006; Devinsky et al., 2018; Palmieri

* Corresponding author.
E-mail address: filippo.maggi@unicam.it (F. Maggi).

https://doi.org/10.1016/j.indcrop.2020.112688
Received 5 March 2020; Received in revised form 2 May 2020; Accepted 8 June 2020

et al., 2019).

The availability of hemp biomass produced during manufacturing and processing of fibre and seeds represents a valuable resource to exploit and valorize on an industrial level. Thus, the increase of hemp cultivation in the years to come may represent an important occasion to valorize the potential of this multipurpose crop by developing innovative products from the huge amount of biomass produced during plant processing (Calzolari et al., 2017). In this regard, the hemp essential oil could be a product of interest for the pharmaceutical, nutraceutical and cosmeceutical industries and useful in integrated pest management (IPM) programs (Fiorini et al., 2019; Benelli et al., 2018a, b). In addition, its production may satisfy the increasing demand for oily extracts from cannabis (Fiorini et al., 2019). The essential oil may act as a good pesticide, notably against aphids, houseflies and ticks (Benelli et al., 2018a, b; Tabari et al., 2020), giving an added value to the whole production chain.

The hemp essential oil is produced in the capitate trichomes that are particularly abundant in inflorescences and, to a minor extent, in leaves (Happyana et al., 2013). The main volatile components can be divided into three groups depending on the cultivar, plant organ, storage, processing and extraction technique: i.e. monoterpenes including α-pinene, myrcene and terpinolene, sesquiterpenes such as (*E*)-caryophyllene, α-humulene and caryophyllene, and cannabinoids with cannabidiol (CBD) as the predominant compound, whereas δ-9-tetrahydrocannabinol (THC) is missing or occurs at trace levels (Mead, 2017; Benelli et al., 2018a, b; Bertoli et al., 2010). Thus, the hemp essential oil is an interesting non-psychotropic product showing a complex mixture, made up of terpenes and cannabinoids, able to produce the so-called 'entourage-effect' (Nahler et al., 2019).

CBD is a non-psychotropic cannabinoid endowed with notable immunomodulatory, anticonvulsant, anti-inflammatory, neuroprotective and anticancer effects (Appendino et al., 2011; Morelli et al., 2014; Russo, 2016; Nabissi et al., 2016; Watt and Karl, 2017; Gertsch, 2018). It acts on CB2 receptors and modulates the psychotropic effects of THC. Noteworthy, it was shown that CBD may defend the plant against herbivore attacks due to its antifeedant properties (Park et al., 2019). (*E*)-caryophyllene is an FDA-approved additive, recently recognized as a ligand of CB receptors with a non-cannabinoid structure. Notably, it is a selective agonist of CB-2 receptors, modulating the inflammatory processes and may also synergize the CBD action (Gertsch, 2008; Chicca et al., 2014; Sut et al., 2018). This sesquiterpene has also been found as an effective mosquitocidal and acaricidal agent (Pavela et al., 2020; Tabari et al., 2020). α-Humulene is reported as an anti-inflammatory and anticancer agent (Legault and Pichette, 2007), and owns insecticidal and acaricidal potential (Benelli et al., 2018c; Tabari et al., 2020). Caryophyllene oxide, the degradation product of (*E*)-caryophyllene, is an FDA-approved food additive owning anticancer activity and synergistic effects with chemoterapics (Fidyt et al., 2016; Hanušová et al., 2017). α-Pinene interacts with the cholinergic system improving memory and learning and counterbalances the toxicity of THC (Lewis et al., 2018). Myrcene has sedative and relaxant effects (Do Vale et al., 2002).

The most common extraction techniques to get essential oil from hemp both at laboratory and industrial scale are steam- (SD) and hydrodistillation (HD). However, they show some disadvantages, e.g., they are time-consuming, request high energy and water input, and sometimes cause thermal degradation of thermosensitive molecules (Filly et al., 2014). In the last years, solvent-free approaches have been designed for the extraction of volatile organic compounds (VOCs) from medicinal and aromatic plants (MAPs). Among them, microwave-assisted extraction (MAE) appears to be an effective, reliable, green technology to improve the extraction of VOCs from different kinds of matrices without the use of organic solvents (Lucchesi et al., 2004). This novel and efficient method works through microwave radiation causing vibration of water and other polar molecules with an increase of temperature and evaporation of water that disrupts cells and matrices with the release of VOCs from the matrix by azeotropic distillation (Filly et al., 2014). In this way, the diffusion of target compounds is easier and faster, saving time and energy. When applied to the extraction of essential oils, MAE revealed to have higher yields and lower costs, compared with conventional techniques such as SD and HD (Filly et al., 2014; Petigny et al., 2014). MAE efficacy is related to the selection of suitable operative conditions. Specifically, for every plant matrix and solvent composition, the effectiveness of the extraction process is dependent on the solvent-to-feed ratio, extraction temperature and time, and microwave irradiation power. Usually, an increase of microwave power and extraction time is associated with an increase of the yield even if this effect tends to level off after certain values. However, excessive heating of the matrices has to be avoided since it could damage some thermosensitive compounds. Concerning the solvent-to-feed ratio, a general trend cannot be defined since the results are strictly related to the matrix and solvent type (Veggi et al., 2012).

Recently, we showed that pretreatment with microwaves or oven heating has a significant effect on modulating the chemical profile of the hemp essential oil, for instance increasing the content of bioactive CBD and (*E*)-caryophyllene (Fiorini et al., 2019). On this basis, we decided to optimize for the first time the MAE process to get a bioactive-enriched essential oil from hemp using the Milestone ETHOS X for the microwave green extraction of natural products (Turk et al., 2018).

For this purpose, a statistical approach, the response surface methodology (RSM) - central composite design (CCD), was applied in order to understand the relationship between the hemp volatile constituents, essential oil yield and extraction parameters. The determined mathematical models were validated and then used to maximize the oil yield and recovery of bioactive compounds such as phytocannabinoids. The RSM methodology proved to be an effective tool in the MAE optimization of the extraction recovery of some essential oils (Petigny et al., 2014; Abedi et al., 2017; Mollaei et al., 2019), although it has been rarely applied for the evaluation of the extraction efficiency on single bioactive compounds. To the best of our knowledge, the optimization of the marker hemp volatile compounds as a function of extraction conditions has never been performed. To complete the work, we also determined the enantiomeric distribution for the main hemp optically active compounds, namely α-pinene, β-pinene, limonene, (*E*)-caryophyllene and caryophyllene oxide, by using chiral chromatography.

2. Materials and methods

2.1. Plant material

Dry inflorescences of hemp were provided by Coop Canapa – Società Cooperativa Agricola, San Severino Marche, Italy (https://www.coopcanapa.it). They were obtained from female individuals of *C. sativa* cv CS (Carmagnola Selezionata) cultivated in Castelbellino (N 43°30′07.80″; E 13°11′16.33″, 200 m a.s.l.) and harvested in October 2018. Hemp inflorescences were dried under darkness at 20 °C and 50 % R.H. until constant weight, afterward they were crushed into small pieces and stored into jute bags until used.

2.2. Microwave-assisted extraction (MAE)

MAE was performed using a Milestone ETHOS X (Milestone, Italy) advanced microwave extraction system (Fig. 1). This is a multimode microwave reactor of 2.45 GHz, equipped with two magnetrons with a maximum delivered power of 1800 W (2 × 950 W) and an infrared sensor monitoring the temperature. The experiments were carried out at atmospheric pressure using a glass reactor (Pyrex) of 5 L capacity closed with a glass cover (Fig. 1). Before extraction dry biomass (500 g) was moistened for 30 min in a vessel filled with 5 L of distilled water, then well-drained and weight to be processed through MAE. The system was configured using the 'Fragrances set-up', consisting of a glass

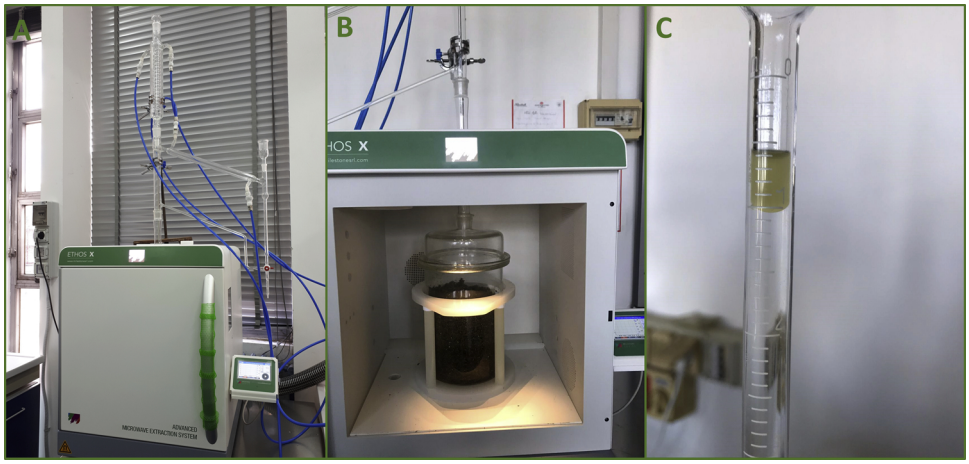

Fig. 1. ETHOS X advanced microwave extraction system (A); glass reactor (Pyrex) of 5 L of capacity (B); hemp essential oil condensed into the graduated burette (C).

Clevenger-type apparatus above the oven, condensing the volatile compounds continuously and allowing water to return inside the reactor. After each extraction run, the essential oil, having a density of 0.893 g/mL, was separated from the water layer and collected in vials sealed with PTFE-silicon septa that were stored at 4 °C until chemical analysis. The essential oil yield was expressed in % (w/w). Three main parameters were optimized during extractions: microwave irradiation power (W/g of moistened biomass), extraction time (min) and water added after moistening (% of moistening biomass).

2.3. Design of the experiments (DoE)

The effect of MAE conditions on the essential oil yield and composition was evaluated by applying a response surface methodology, specifically a central composite design. For a three factors study as in this case, a CCD is composed by:

- 8(2^3) factorial experiments, designated by the coded variables -1 or 1.
- 6 (2*3) axial experiments, defined by the coded variables -1.682 or +1.682.
- 4 central experiments, specified by the coded variable 0.

The presence of the 6 axial points set at 1.682 in addition to a 2^3 full factorial design assures the obtaining of a spherical experimental domain and design rotatability. Moreover, the 4 central points guarantee uniform precision within the experimental domain (Lewis et al., 1999a).

The complete list of all the 18 extractions runs with the corresponding coded and uncoded variables is reported in Table 1. Each extraction run was characterized in terms of:

- Essential oil yield (%), calculated as follow:

$$EO\ yield\ (\%) = \frac{weight\ of\ EO\ (g)}{weight\ of\ dry\ biomass\ (g)} \cdot 100$$

- Concentration of hemp marker volatile compounds (g/100 g of essential oil), determined by GC-FID as reported in the section 2.4.

In the DoE terminology the essential oil yield and the concentration of bioactive compounds represent the responses of the design while the microwave irradiation power, extraction time and water added after moistening are the design variables or factors.

2.4. Quantification of the marker compounds by GC-FID analysis

Quantification of α-pinene, myrcene, terpinolene, (*E*)-caryophyllene, α-humulene, caryophyllene oxide and CBD in the hemp essential oil was performed by means of gas chromatography coupled with flame ionization detection (GC-FID) using an Agilent 6850 GC series. Analytical standards of the above compounds were purchased from Sigma-Aldrich (Milan, Italy). The hemp essential oil was diluted with analytical grade *n*-hexane (6 µL in 594 µL of *n*-hexane) and 0.5 µL injected in split mode (split ratio 1:30) into the GC. The injector temperature was 300 °C. The carrier gas was hydrogen produced by a generator PGH2 – 250 from DBS Analytical Instruments, Vigonza, Italy. The initial gas flow in the column was 3.7 mL/min. Chromatography was performed on a 5%-phenyl-methylpolysiloxane coated capillary column (HP-5, 30 m l., 0.32 mm i.d., 0.25 µm f.t., Agilent Technologies). The oven temperature was held at 60 °C for 3 min, then raised until 350 °C at 25 °C/min and held for 1 min, for a total run time of 15.60 min. The FID temperature was set at 360 °C, and hydrogen and air flow were 40 and 400 mL/min, respectively. The quantification was performed by using the calibration curves obtained for α-pinene, myrcene, terpinolene, (*E*)-caryophyllene, α-humulene, caryophyllene oxide and CBD which were built by preparing stock standard solutions at 7 different concentrations in the range 0.004–9.6 mg/mL. Correlation coefficients ranged from 0.9991 to 0.9998. β-Pinene and (*E*)-β-ocimene were quantified using the calibration curve obtained for α-pinene; limonene and 1,8-cineole were quantified by the terpinolene calibration curve.

2.5. GC–MS analysis

The study of essential oil chemical profiles was carried on an Agilent 6890 N GC-MS system equipped with a 5973 N single quadrupole detector and an autosampler 7863 (Agilent, Wilmingotn, DE). The capillary column used for separation of peaks was coated with 5% phenylmethylpolysiloxane (HP-5MS, 30 m l. × 0.25 mm i.d., 0.1 µm f.t., Agilent). The oven was thermostatted at 60 °C for 5 min, then ramp at 4 °C/min up to 220 °C, finally ramp at 11 °C/min to 280 °C, isothermal for 15 min. Injector and detector temperatures were 280 °C. The carrier gas was He (99.5 %) flowing at 1 mL/min. The oils were diluted 1:100 in analytical-grade *n*-hexane (Sigma-Aldrich) and injected in split-mode with a split ratio of 1:50. The mass spectra were acquired in full scan in the range 29.0–400.0 uma using the electron ionization (EI) mode with an electron energy of 70 eV. For the peak assignment, the MSD ChemStation (Agilent, Version G1701DA D.01.00) and the NIST Mass Spectral Search Program were used. The identification of the major components was carried out by co-injection with authentic standards

Table 1
MAE conditions for all the 18 runs performed according to the central composite design (CCD). The set of each single factor is reported both as coded and uncoded variables.

Run	Point type[a]	Coded variables			Uncoded variables		
		Microwave power	Extraction time	Water	Microwave power (W/g)	Extraction time (min)	Water (%)
1	F	−1	−1	−1	0.8	60.0	35.0
2	F	+1	−1	−1	1.1	60.0	35.0
3	F	−1	+1	−1	0.8	100.0	35.0
4	F	+1	+1	−1	1.1	100.0	35.0
5	F	−1	−1	+1	0.8	60.0	55.0
6	F	+1	−1	+1	1.1	60.0	55.0
7	F	−1	+1	+1	0.8	100.0	55.0
8	F	+1	+1	+1	1.1	100.0	55.0
9	A	−1.682	0	0	0.7	80.0	45.0
10	A	+1.682	0	0	1.2	80.0	45.0
11	A	0	−1.682	0	0.95	46.4	45.0
12	A	0	+1.682	0	0.95	113.6	45.0
13	A	0	0	−1.682	0.95	80.0	28.2
14	A	0	0	+1.682	0.95	80.0	61.8
15	C	0	0	0	0.95	80.0	45.0
16	C	0	0	0	0.95	80.0	45.0
17	C	0	0	0	0.95	80.0	45.0
18	C	0	0	0	0.95	80.0	45.0

[a] This column defines, for each experimental condition, whether a Factorial (F), Axial (A) or Central (C) point is represented.

(Sigma-Aldrich). In addition, we calculated the temperature-programmed retention indices (RIs) according to Van den Dool and Kratz (1963) formula:

$$RIx = 100n + 100(tx - tn)/(tn + 1 - tn)$$

where n is the carbon atoms of the alkane eluting before the peak, t_n and t_{n+1} are the retention times (RTs) of the alkanes eluting before and after the peak, and t_x is the RT of the peak to be assigned. The coherence of RI was overlapped with the MS matching using the ADAMS, NIST 17, FFNSC3 and WILEY275 libraries (Adams, 2007; NIST 17, 2017; FFNSC3, 2015). The relative content of peaks was determined by normalization of peak areas without using response factors.

2.6. Central composite design analysis

2.6.1. Model determination and analysis

For each single response, all the results of the 18 runs were analyzed by multilinear regression using a full quadratic model:

$$y = \beta_0 + \sum_{i=1}^{n} \beta_i \bullet x_i + \sum_{i=1}^{n} \beta_{ii} \bullet x_i^2 + \sum_{i<j}^{n} \beta_{ij} \bullet x_i x_j$$

Where y is the response, β_0 is the model constant, β_i is the coefficient corresponding to the variables x_i (linear terms), β_{ii} are the coefficients associated with the variables x_{ii} (quadratic term) and β_{ij} are the coefficients associated with the variables x_{ij} (first-order interaction terms).

The fitting of the full quadratic model generates a large set of explanatory variables (the coefficients) and the equation could suffer from some degree of multicollinearity, with consequent biased parameters and sometimes with the wrong sign, and from poor prediction ability (overfitting) (Chatterjee and Simonoff, 2013). For these reasons, all the generated full quadratic models were subjected to a variable selection procedure (model reduction) in order to improve the precision of the estimated coefficients of the retained variables, minimize the mean square error and, more in general, satisfy the principle of parsimony (Forster, 2000; Chatterjee and Simonoff, 2013).

The model reduction has been performed by stepwise regression in backward elimination mode. This procedure carried out a sequence of fit beginning with the model containing all the predictors, and then iteratively removing the least useful predictor (i.e., the one with the lowest p-value), one-at-a-time. Among all the sets of generated models, the best one has been selected by evaluating the adjusted coefficient of multiple determination (R^2_{adj}), the predicted coefficient of multiple determination (R^2_{pred}) and the Mallows' Cp statistic (Zuccaro, 1992; Minitab blog, 2013; Chatterjee and Simonoff, 2013).

The selected models were then evaluated through ANOVA, coefficient and residual analysis.

The model fitting, selection and analysis has been performed with the Minitab 18 statistical software.

2.6.2. MAE optimization and model validation

The models developed as reported in the previous section allow to understand the relationships between the factors and every single response and to map the experimental domain. Such information is enough to define the best operative conditions only for every single response. However, in the presence of more responses, as in this case, it is necessary to identify the more suitable experimental conditions able to provide satisfactory results for all the responses at the same time (multiple responses optimization). The multiple responses optimization has been performed using the desirability method. For every single response, a partial desirability function (Dp) varying from 0 (completely unsatisfactory results) to 1 (completely satisfactory results) has been identified. All the Dp are then combined together calculating the geometric mean, which represents the composite desirability function D. Similarly, D ranges between 0 (at least one response is completely unsatisfactory) and 1 (all the responses are completely satisfactory) (Lewis et al., 1999b; Minitab 18 Support a, 2020).

For the optimization of yield and CBD responses, a linear partial desirability function that maximizes the responses has been chosen, setting the target values and the unacceptable limits as a function of the possible results obtainable in the experimental domain investigated.

Together with the optimized conditions, namely those with the highest D value, a further set of conditions having low D and consequently low performance has also been identified. These two set of variables were named V1 and V2, respectively. The conditions V1 and V2 were experimentally applied during MAE and their essential oil yield and CBD content determined as for all the runs of the CCD sequence. The experimental values of V1 and V2 were then compared with those predicted by the models (predicted fit values and 95 % prediction interval) (Minitab 18 Support b, 2020).

Multiple responses optimization (desirability), as well as the calculus of the 95 % prediction intervals for a certain predicted value, were carried out using the software Minitab 18. The MAE extractions V1 and V2 were performed in triplicate.

Table 2
Model Evaluation: coefficients of determinations (R^2_{adj} R^2_{pred}), Mallows' Cp statistic and ANOVA results.

Response	Best model[#]	R^2	R^2_{adj}	R^2_{pred}	Mallows' Cp	P-Value Regression[$]	P-Value Lak of fit[$]
Yield (%)	Y = -0.0889 + 0.0902 P + 0.0028 T -0.0008 W – 0.000012 T^2	0.790	0.726	0.595	2.46	***	ns
α-Pinene (g/100 g)	None	> 0.001	> 0.001	> 0.001	/	/	/
β-Pinene (g/100 g)	Y = 1.465 + 0.0.18W	0.094	0.037	> 0.001	−4.97	ns	ns
Myrcene (g/100 g)	Y = -12.8 + 0.2 T +0.045W-0.004 TW	0.324	0.179	> 0.001	−0.6	ns	ns
Limonene (g/100 g)	Y = 2.44 − 1.146 P +0.026W	0.275	0.178	> 0.001	−1.7	ns	ns
1,8-Cineole (g/100 g)	Y = 0.533 + 0.009W	0.173	0.120	0.035	−5.05	ns	ns
Terpinolene (g/100 g)	Y = -6.3 + 0.09 T +0.182W-0.002 TW	0.399	0.270	0.059	2.7	ns	ns
(*E*)-Caryophyllene (g/100 g)	Y = -96.4 + 218.7 P + 0453 T +0,4 W – 1.357 P T - 2.17 P W + 0.017TW	0.622	0.415	> 0.001	4.60	ns	ns
α-Humulene (g/100 g)	Y = -13.1 + 34.3P + 0.34 T -0118 W – 0.383PT	0.379	0.188	> 0.001	2.25	ns	ns
Caryophyllene oxide (g/100 g)	Y = 13.1–23 P - 0176 T -0.173 W +0.481 P W - 0.003PW	0.375	0.114	> 0.001	3.34	ns	ns
CBD (g/100 g)	Y = -22.4 + 57.5 P + 004 T -0072 W – 26.8P^2	0.771	0.701	0.611	1.77	***	ns

[#] The models are reported using the coefficients calculated from the uncoded variables. The abbreviations in the models are as follows: P for microwave power, T for extraction time, W for water. The quadratic terms are represented by the quadratic exponent (i.e.. T^2), while the interactions terms by the product of two linear terms (i.e. TW). [$]The results of P-value columns are reported as follows: ns = $p > 0.05$; * $0.05 < p < 0.01$; ** $0.01 < p < 0.001$; *** $p < 0.001$.

2.7. Hydro-distillation (HD)

In order to compare the extraction efficiency of MAE with respect to conventional hydrodistillation (HD), 500 g of dry inflorescences were inserted into a 10 L flask equipped with a mantle system Falc MA (Falc Instruments, Treviglio, Italy) and 5 L of deionized water were inserted. Afterward, HD was made by a glass Clevenger-type apparatus for 240 min. This extraction time was selected based on previous works (Benelli et al., 2018a, b; Fiorini et al., 2019). At the end of the process, the essential oil, having a density of 0.886 g/mL, was collected in vials equipped with PTFE-silicon septa and stored at 4 °C until chemical analysis. The essential oil yield was determined as reported in sect. 2.3.

2.8. Enantioselective GC-MS analysis

The chiral analysis was carried out using the same GC–MS apparatus reported above (sect. 2.5.), equipped with a HP-Chiral 20β [20% β-cyclodextrin in (35%-phenyl)-methylpolysiloxane, 30 m l. × 0.25 mm i.d., 0.25 μm f.t.] capillary column which was purchased from Agilent. The oven temperature was programmed as follows: initial temperature of 50 °C, rising to 220 °C at 2 °C/min then isotherm for 1 min. Inlet temperature was set to 250 °C, whereas the MS quad and source temperatures were 150 and 250 °C, respectively. The carrier gas was helium with a flow of 1 mL/min. The essential oil was diluted 1:100 in *n*-hexane and the injected volume was 1 μL with a split ratio of 1:50. The mass acquisition parameters were set up as in the sect. 2.5. The optically active isomers of α-pinene, β-pinene, limonene, (*E*)-caryophyllene and caryophyllene oxide were identified by comparison of RT and RI (calculated respect to a mixture of C_7-C_{30} *n*-alkanes, Sigma-Aldrich) with those of analytical standards (Sigma-Aldrich) chromatographed under the GC conditions described above. Their relative content was determined by computing the peak area percentage.

3. Results and discussion

In the present study, we optimized for the first time the extraction of the hemp essential oil using the ETHOS X, developed and patented by Milestone. This device showed to maximize the volatile terpenes and terpenoids extraction from the Cannabis plant, maintaining THC and CBD's content in the fresh plant matrix (Milestone srl, 2019). Indeed, this procedure works well when the fresh inflorescences are used. In this case, the essential oil is devoid or contain trace levels of cannabinoids (Bertoli et al., 2010; Benelli et al., 2018b; Iseppi et al., 2019). However, if the plant material is subjected to drying before extraction, decarboxylative reactions occurring during this stage (Fiorini et al., 2019) may contribute to increasing the recovery of cannabinoids, and this may be boosted by the MAE process. On this basis, we optimized the operative conditions for MAE using dry female inflorescences obtained from the Italian hemp variety CS (Carmagnola Selezionata).

3.1. DoE analysis

The analysis of MAE process using a CCD approach requires the identification of suitable mathematical models able to describe how the extraction experimental conditions (factors) influence the measured responses (essential oil yield and concentration of bioactive compounds in the essential oil). The best models for each response are reported in Table 2 together with the parameters used for the model selection, R^2_{adj} R^2_{pred} and Mallows' Cp statistic. Interestingly, only two responses could be properly modeled, the yield and the CBD concentration. For all the other cases, the very low values of R^2_{adj} and R^2_{pred} suggest as all the tested models were completely unsuitable. In one case, i.e. α-pinene concentration, we were unable to identify a model (all the evaluated models possessed a R^2_{adj} lower than 0.001). In all these cases, since both the lack of fit and regression were not significant (Table 2), it can be concluded that the response variations among all the experimental runs can be mainly attributed to intrinsic variability. On the other side, for the oil yield and CBD concentration, the model is adequate (lack of fit not significant) and describes most of the variability observed (regression significant). In addition, for both responses the residual analysis (Figures 1SM and 2SM, Supplementary Material) did not highlight any violation of the assumptions of regression, while the coefficient analysis excluded the issue of multicollinearity (correlation between predictors) of the model (Table 1SM, Supplementary Material).

The identification of a suitable model for the yield and CBD concentration allows understanding the relationships between the factors and responses and even to map response variation inside the experimental domain. The effect of each single factor on a single response can be easily visualized using the main effect plots (Fig. 2). For both responses, all the factors work in the same direction, even if in a quantitative and qualitative different manner, with microwave power and extraction time that increase the oil yield and CBD content, while the amount of water added acts in the opposite direction. It has also to be highlighted that the microwave power and extraction time possess the strongest effect, especially for the yield, compared with water. The global effect of all variables together can be instead observed using surface plots (Fig. 3). These graphs were built setting the value of the less relevant factor, i.e. water, to the coded value of 0 (corresponding to

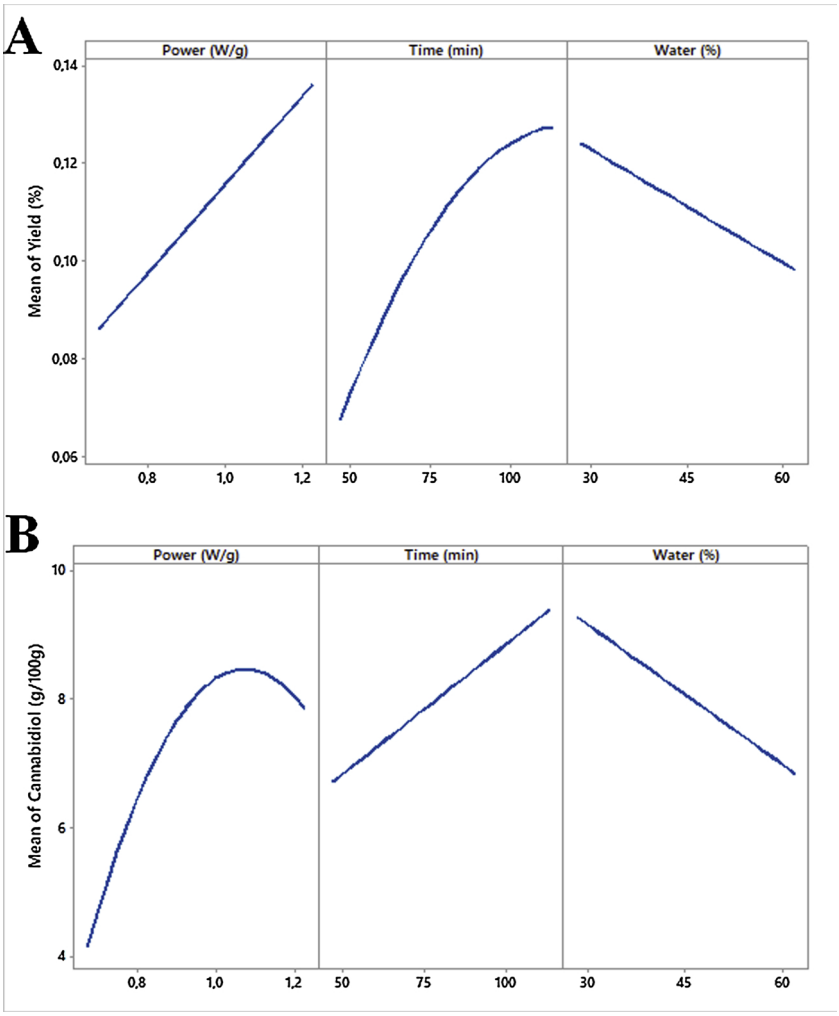

Fig. 2. Main effect plots showing the effect of each factor on the (A) yield (%) and the (B) CBD concentration.

45 % for the uncoded value). However, since for the factor water only the linear terms are significant, a variation of the water amount would simply determine a shift of the surface along the z axis (i.e., that of the response), without any change in the shape and intensity of the curvature. The surface plot for the yield (Fig. 3A) is characterized by a low curvature and point out as the highest yield can be recovered working at high microwave irradiation power and long extraction times, keeping the water percentage added at the lowest level. Concerning the CBD, the surface plot is slightly more complex, due to the higher relevance of the quadratic term of microwave power. In this case, the surface (Fig. 3B) shows a more marked curvature and the highest concentrations were obtained using long extraction times at moderately high irradiation power (around 1.1 W/g). Also in this case, water displayed the same effect observed for the yield.

An interesting aspect regards how the single bioactive components in the essential oil are related to the yield. In this respect, DoE analysis seems to suggest as an increase in the yield could be due to an increase in the recovery of CBD. To test this hypothesis a Pearson correlation analysis has been performed between the yield and the concentration of all the bioactive components quantified by GC-FID. The results showed as only CBD has a moderate positive correlation with the yield, resulting in a statistically significant (P-value of 0.0084) correlation coefficient of 0.6 (Fig. 4). For all the other components the correlation was very weak (always lower than 0.4) and never statistically significant (Table 2SM, Supplementary Materials). This may be explained by the fact that the plant material suffered from partial evaporation of more volatile mono- and sesquiterpenes during drying. Thus, it results as the yield variation during the 18 experimental runs is partially due to a concomitant variation of the CBD content.

3.2. MAE optimization and model validation

The yield and CBD content were contemporaneously optimized using the Desirability approach. In both cases, the two responses were maximized, and the global desirability function was plotted in Fig. 5. The higher desirabilities can be obtained using microwave power values around 1.1 W/g and extraction times of about 115 min, while for microwave power values lower than 0.9 W/g and extraction times lower than 60 min the desirability was 0, indicating an unacceptable low result in terms of yield and/or CBD concentration. To validate the models, two further extractions, V1 and V2, were carried out setting the MAE conditions in order to obtain the highest and lowest desirability (D = 1 and 0, respectively). The MAE experimental conditions, the predicted values and the 95 % interval of predictions are reported in Table 3. The comparison between the predicted values and those experimentally obtained, reported in Fig. 6, demonstrates the validity of the models in the prediction of the performance of MAE for hemp. According to the optimized process, the highest essential oil yield and CBD content were 0.15 ± 0.04 and 9.33 ± 0.69 %, respectively.

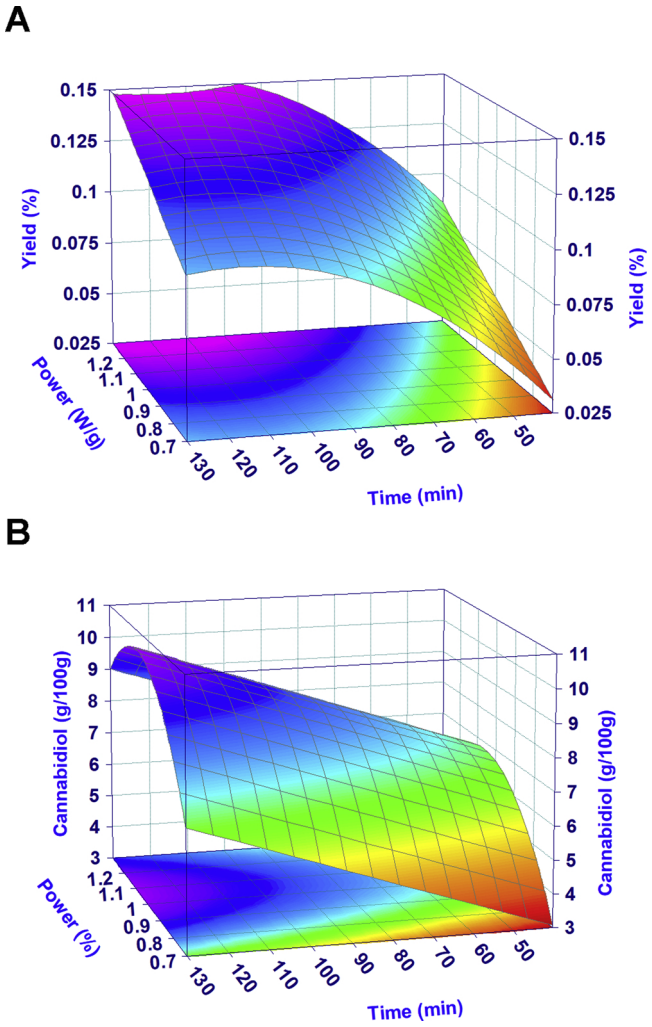

Fig. 3. Surface plots for the (A) yield (%) and the (B) CBD concentration. The plots show the effect of microwave irradiation power and extraction time at a fixed level of water, 45 % (coded value 0).

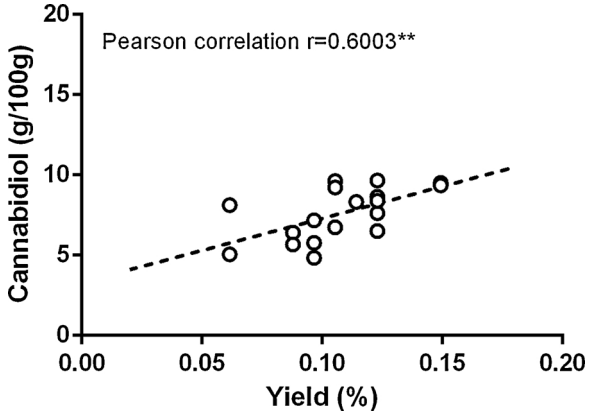

Fig. 4. Correlation between yield (%) and CBD concentration.

3.3. DoE analysis comparison using GC-FID and GC–MS data

The DoE analysis and optimization has been carried out using the GC-FID quantitative method (sect. 2.4). However, in the essential oil analysis it is common to present semi-quantitative data obtained at GC–MS (Pavela et al., 2017). Therefore, we decided to investigate the reliability of GC–MS semi-quantitative data in DoE analysis and optimization. Firstly, a Pearson correlation analysis has been performed between all the monitored bioactive compounds concentrations determined by both methods for each run of the CCD. The results highlight a strong correlation, always statistically significant, for all the compounds (Pearson $r \geq 0.92$ and P-value ≤ 0.0001) (Table 3SM, Supplementary Materials). The only exception was found for the α-humulene, which showed a lower correlation (Pearson r equal to 0.735) though highly significant (P-value equal to 0.0005). Thus, from a qualitative point of view (in terms of analyte response to diverse extractive conditions) the two analytical techniques can be considered equivalent. Subsequently, we analyzed the DoE replacing the GC-FID data with the ones from GC–MS. As observed in Table 4SM, Supplementary Materials, the model analysis results almost equivalent. Also in this case, only the CBD model described properly the experimental data. It is worth noting that the model parameters of CBD obtained using GC–MS data are exactly the same of those detected using the GC-FID method. The only difference is the slightly better descriptive capacity of the latter (in terms of R^2_{adj} and R^2_{predj}). A visual comparison of the two models can carried out using the contour plots as reported in Fig. 3SM, Supplementary Materials.

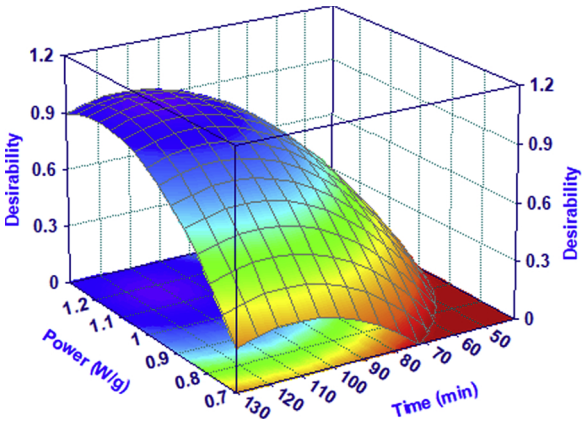

Fig. 5. Surface plots of the desirability. The plots show the effect of microwave irradiation power and extraction time at a fixed level of water, 35 % (coded value -1).

3.4. Comparison of essential oil chemical profiles obtained by HD and MAE

Overall, both HD and MAE (V1 optimized sample) yielded similar amounts of oils, namely 0.14 and 0.15 %, respectively. However, MAE reduced the whole extraction time to only 115 min compared with 240 min needed for HD.

Table 4 reports the chemical composition of the essential oils obtained from hemp inflorescences subjected to HD and MAE. As concerning the chemical profiles obtained, no qualitative differences were observed in the two chromatograms as determined by GC–MS (Fig. 7). Overall, a total of 71 components were identified in the two oils, accounting for 91.0–92.0 % of the total compositions. The main fraction of the oils was given by sesquiterpene hydrocarbons, followed by monoterpene hydrocarbons, cannabinoids, oxygenated sesquiterpenes and oxygenated monoterpenes. The main constituents in both essential oils (in decrescent order of relative abundance) were (*E*)-caryophyllene, CBD, *α*-humulene, *α*-pinene, caryophyllene oxide and myrcene. These chemical profiles were qualitatively overlapping, at least for the major terpenoid constituents, with those previously reported by other authors

Table 3
MAE experimental conditions, desirabilities, predicted values and the 95 % interval of predictions of the two validation runs (V1 and V2) for the Yield and CBD model.

Extraction	MAE conditions			Desirability	Response	Predicted value	95 % interval of prediction
	Power (%)	Time (min)	Water (%)				
V1	1.05	113.6	28.2	1	Yield %	0.149	0.112 – 0.186
					CBD (g/100 g)	11.0	8.65 – 13.36
V2	0.85	65	50	0	Yield %	0.082	0.052 – 0.111
					CBD (g/100 g)	6.15	4.09 – 6.91

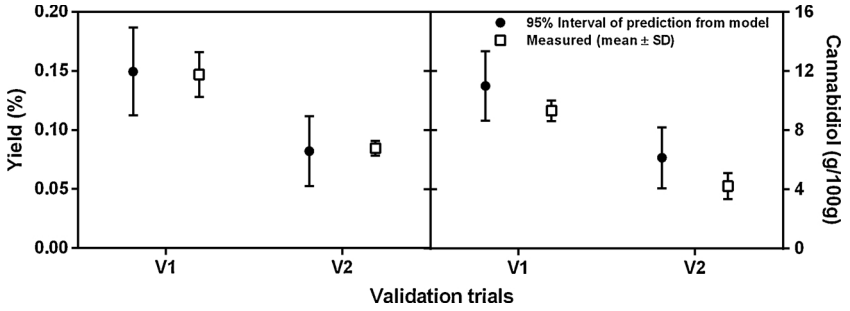

Fig. 6. Comparison between predicted and experimental results of the two validation runs V1 and V2. The predicted results are reported as predicted value and 95 % interval of prediction.

for the same and other hemp cultivars (Bertoli et al., 2010; Benelli et al., 2018a; Iseppi et al., 2019).

It is worth mentioning the occurrence in both essential oils of trace amounts of other cannabinoids such as cannabidivarol, cannabicitran, cannabichromene and THC.

When comparing the two extraction techniques using the GC-FID quantification method, MAE resulted more effective than HD in yielding higher amounts of CBD (9.3 vs 5.6 %, respectively) as well as those of the main sesquiterpenes (*E*)-caryophyllene and *α*-humulene (46.5 vs 36.1 %, and 18.8 vs 14.2 %, respectively). On the other hand, the amounts of the main monoterpenes were higher in the HD sample (Fig. 8). The increase in the CBD content in MAE may be related to the higher energy penetration of microwaves boosting the decarboxylative reactions into the plant matrix that convert cannabidiolic acid into the respective alcoholic form. In addition, the high energy provided to the plant matrix alter the quantitative ratio of the terpene profile by favouring the extraction of the high-boiling point sesquiterpenes over the low boiling-point monoterpenes. Indeed, during MAE more energy is given to the system so that some of the more volatile compounds can be lost due to overheating of the vapor.

The hemp essential oils obtained using both extraction techniques are endowed with a complex composition in which a couple of bioactive compounds such as the phytocannabinoids (*E*)-caryophyllene and CBD appear to be the most important ones. In this respect, MAE appears to be more selective than HD for CBD. Notably, MAE increased the recovery of CBD from the plant matrix with shorter extraction times and reduced costs related to energy and water consumption (Filly et al., 2014). Thus, the chemical profile obtained appears to be interesting since (*E*)-caryophyllene, a dietary phytocannabinoid with a non-cannabinoid structure, is able to synergize the action of CBD as reported by some authors (Russo, 2011; Fine and Rosenfeld, 2013). On the other hand, the remaining fraction of the hemp essential oil, composed of monoterpene hydrocarbons (α-pinene, myrcene and terpinolene) and sesquiterpenoids (α-humulene and caryophyllene oxide), may contribute to give the so-called 'entourage effect' to the final product. Thus, the potential applications of the CBD-enriched hemp essential oil should be assessed in future studies.

3.5. Enantiomer distribution of chiral components

In the present study we assessed for the first time the enantiomeric distribution and excess (EE) of chiral constituents in hemp essential oil obtained by MAE in order to determine its organoleptic and chemical-biological properties.

The enantiomers of *α*-pinene, *β*-pinene, limonene, (*E*)-caryophyllene and caryophyllene oxide were successfully separated by a chiral column (HP 20β) and identified using GC–MS (Table 5). Notably, the order of elution of the enantiomers of α-pinene and β-pinene was consistent with that of a study where the same chiral stationary phase was used (Dahmane et al., 2015). The three monoterpenes were found as enantiomeric pairs, whereas the two sesquiterpenes [(*E*)-caryophyllene and caryophyllene oxide] were exclusively present as the (-)-enantiomer form. For α-pinene the EE was 90.17 %, with the predominance of the (+)-*α*-pinene enantiomer; for *β*-pinene the EE was 74.17 %, with the prevalence of the (+)-*β*-pinene enantiomer; for limonene the EE was 86.50 %, with (+)-limonene being the most prevalent enantiomer. It is worth mentioning that the (+)-enantiomers of *α*- and *β*-pinene showed higher biological activity than the (-)-enantiomers (Silva et al., 2012).

The enantiomers occurring in the hemp essential oil have different aroma descriptors. (-)-*α*-Pinene has a slightly minty scent, whereas the (+) enantiomer has a pine-like odor; the (+)-limonene owns a citrus-like note whereas the (-)-limonene has a turpentine-like smell; *β*-pinene has a woody-pine smell (Bordiga and Nollet, 2019). (-)-(*E*)-caryophyllene has a weak woody-spicy odor (Gertsch, 2008). (-)-Caryophyllene oxide is the key component responsible for marijuana and hashish detection by police dogs (Stahl and Kunde, 1973).

4. Conclusions

In the last years, the global market of CBD and hemp derivatives is continuously growing, acquiring importance from multiple standpoints, namely economics, medicine, industry and agriculture. This has been reflected by a significant increase in hemp cultivation area worldwide. In the US, the market of CBD accounted for 200 mln $ in 2017 and is

Table 4
Chemical composition of the hemp essential oils obtained by HD and MAE.

N	Component[a]	RI[b]	RI LIT.[c]	Relative peak area (%)		ID[d]
				HD	MAE (V1)	
1	2-heptanone	892	889	tr[e]	tr	RI,MS
2	heptanal	903	901	0.1	0.1	RI,MS
3	5,5-dimethyl-1-vinylbicyclo[2.1.1]hexane	914	920	0.1	0.2	RI,MS
4	*α*-thujene	921	924	tr	Tr	RI,MS
5	*α*-pinene	926	932	5.5 (12.7)[f]	6.0 (10.1)	Std
6	camphene	939	946	0.1	0.1	Std
7	sabinene	966	969	tr	tr	Std
8	*β*-pinene	968	974	1.6 (3.6)	1.5 (2.3)	Std
9	myrcene	989	988	6.1 (13.8)	5.0 (4.7)	Std
10	*α*-phellandrene	1003	1002	0.1	0.1	Std
11	*δ*-3-carene	1007	1008	0.1	tr	Std
12	*α*-terpinene	1014	1014	0,1	0.1	Std
13	*p*-cymene	1021	1020	0.2	0.2	Std
14	limonene	1025	1024	2.1 (4.6)	1.9 (1.8)	Std
15	1,8-cineole	1026	1026	0.8 (1.9)	0.9 (0.7)	Std
16	(*Z*)-*β*-ocimene	1037	1032	tr	tr	Std
17	(*E*)-*β*-ocimene	1046	1044	0.4 (1.2)	0.3 (0.8)	Std
18	γ-terpinene	1055	1054	0.2	0.2	Std
19	*cis*-sabinene hydrate	1063	1065	0.1	0.1	RI,MS
20	terpinolene	1084	1086	2.7 (5.2)	2.0 (1.0)	Std
21	*p*-cymenene	1086	1089	0.1	0.1	RI,MS
22	*trans*-sabinene hydrate	1095	1098	0.1	0.1	RI,MS
23	linalool	1100	1095	0.6	0.5	Std
24	*endo*-fenchol	1108	1114	0.7	0.7	RI,MS
25	*trans*-pinene hydrate	1115	1119	0.3	0.4	RI,MS
26	*trans*-pinocarveol	1133	1135	0.1	0.1	Std
27	borneol	1160	1165	0.2	0.2	Std
28	terpinen-4-ol	1172	1174	0.5	0.5	Std
29	*p*-cymen-8-ol	1183	1179	0.1	tr	RI,MS
30	*α*-terpineol	1186	1186	0.8	0.9	Std
31	*α*-ylangene	1363	1373	0.2	0.1	RI,MS
32	*α*-copaene	1367	1374	tr	tr	RI,MS
33	(*Z*)-caryophyllene	1397	1408	0.2	0.2	RI,MS
34	(*E*)-caryophyllene	1410	1417	22.5 (36.1)	22.2 (46.5)	Std
35	*α*-*trans*-bergamotene	1431	1432	0.6	0.4	RI,MS
36	*α*-guaiene	1431	1437	0.6	0.3	RI,MS
37	6,9-guaiadiene	1436	1442	0.1	tr	RI,MS
38	*α*-humulene	1443	1452	8.9 (14.2)	9.1 (18.8)	Std
39	*allo*-aromadendrene	1450	1458	0.5	0.5	RI,MS
40	(*E*)-*β*-farnesene	1456	1454	0.2	0.2	Std
41	γ-muurolene	1469	1478	tr	tr	RI,MS
42	selina-411-diene	1475	1476	0.7	0.8	RI,MS
43	*β*-selinene	1475	1489	2.2	2.2	RI,MS
44	valencene	1485	1496	0.6	0.7	RI,MS
45	*α*-selinene	1485	1498	1.8	1.7	RI,MS
46	*α*-bulnesene	1497	1509	0.8	0.8	RI,MS
47	*δ*-amorphene	1499	1511	tr	tr	RI,MS
48	*β*-bisabolene	1506	1505	0.3	0.2	RI,MS
49	7-*epi*-*α*-selinene	1506	1520	0.3	0.2	RI,MS
50	δ-cadinene	1516	1522	0.1	0.1	RI,MS
51	selina-4(15),7(11)-diene	1524	1544	0.8	0.8	RI,MS
52	selina-3,7(11)-diene	1530	1538	2.2	2.2	RI,MS
53	*α*-calacorene	1534	1544	0.2	0.3	RI,MS
54	(*E*)-*α*-bisabolene	1540	1544	0.2	0.2	RI,MS
55	(*E*)-nerolidol	1562	1561	0.8	0.8	Std
56	caryophyllene oxide	1571	1583	5.2 (6.6)	5.9 (6.8)	Std
57	humulene epoxide I	1587	1587	0.3	0.3	RI,MS
58	viridiflorol	1591	1592	0.1	0.1	RI,MS
59	humulene epoxide II	1597	1608	1.9	2.0	RI,MS
60	caryophylla-4(12),8(13)-dien-5*α*-ol	1626	1639	0.8	0.6	RI,MS
61	caryophylla-4(12),8(13)-dien-5*β*-ol	1632	1639	0.3	0.4	RI,MS
62	*α*-bisabolol	1678	1685	0.5	0.4	Std
63	eudesm-7(11)-en-4-ol	1684	1700	0.7	0.6	RI,MS
64	hexahydrofarnesyl acetone	1844	1845	0.3	0.4	RI,MS
65	cannabidivarol	2209	2208	0.1	0.1	RI,MS
66	cannabicitran	2260	2261[g]	0.2	0.2	RI,MS
67	cannabidiol	2420	2430[g]	11.5 (5.6)	14.5 (9.3)	Std
68	cannabichromene	2442	2440[g]	0.2	0.3	RI,MS
69	*δ*-9-tetrahydrocannabinol	2535	2529[g]	0.2 (0.1)	0.2 (0.1)	RI,MS
70	*n*-heptacosane	2700	2700	tr	tr	Std
71	*n*-nonacosane	2900	2900	tr	tr	Std
	Oil yield (%, w/w)			0.14	0.15	
	Total identified (%)			91.0	92.9	
	Grouped compounds (%)					
	Monoterpene hydrocarbons			19.4	17.8	
	Oxygenated monoterpenes			4.3	4.3	
	Sesquiterpene hydrocarbons			44.0	43.0	
	Oxygenated sesquiterpenes			10.6	11.0	
	Cannabinoids			12.2	16.3	
	Others			0.4	0.6	

[a] Order of elution is from an HP-5MS column (30 m x 0.25 mm, 0.1 mm).
[b] Linear retention index according to Van den Dool and Kratz (1963).
[c] RI taken from ADAMS and/or NIST 17 and FFNSC3 libraries.
[d] Identification method: Std, comparison with analytical standard; RI, coherence of the calculated RI with those stored in ADAMS, NIST 17 and FFNSC3 libraries. MS, mass spectrum overlapping with those recorded in ADAMS, NIST 17, WILEY 275 and FFNSC3 libraries.
[e] Traces, relative % < 0.1.
[f] Quantitative values obtained at GC-FID.
[g] RI taken from Nagy et al. (2019).

expected to increase further, with a prediction of 450 mln $ in 2020. Noteworthy, the European Union is destined to become the largest world market for hemp derivatives, and several companies have invested more than 500 mln $ in manufacturing different kinds of products (The European Cannabis Report, https://prohibitionpartners.com). The request for CBD has stimulated the search for innovative, green and effective extraction methods. In this respect, the huge amount of by-products produced during hemp fibre processing and manufacturing may represent an important and cheap source for the production of valuable products such as CBD-rich essential oils. The latter may be appealing for the pharmaceutical, nutraceutical, cosmeceutical and agrochemical industries due to the presence of valuable bioactive constituents (Di Pierro, 2015; Lodzki et al., 2003; Scuderi et al., 2009; Russo, 2011; Jastrząb et al., 2019; Park et al., 2019). Most of them, such as CBD and terpenoids, are considered safe, being included in the EU database on 'food flavourings' or in that of US GRAS substances (Russo, 2011). The findings of the present study revealed that MAE is a valid, time- and cost-saving technique for the production of bioactive hemp essential oils with high content of CBD and (*E*)-caryophyllene. Notably, the MAE operative conditions play a crucial role in boosting the CBD content into the final product. The potential of this product to be exploited in different commercial applications should be evaluated in future studies. The manufacture of CBD-enriched essential oils may represent an added value for the implementation of the hemp production chain.

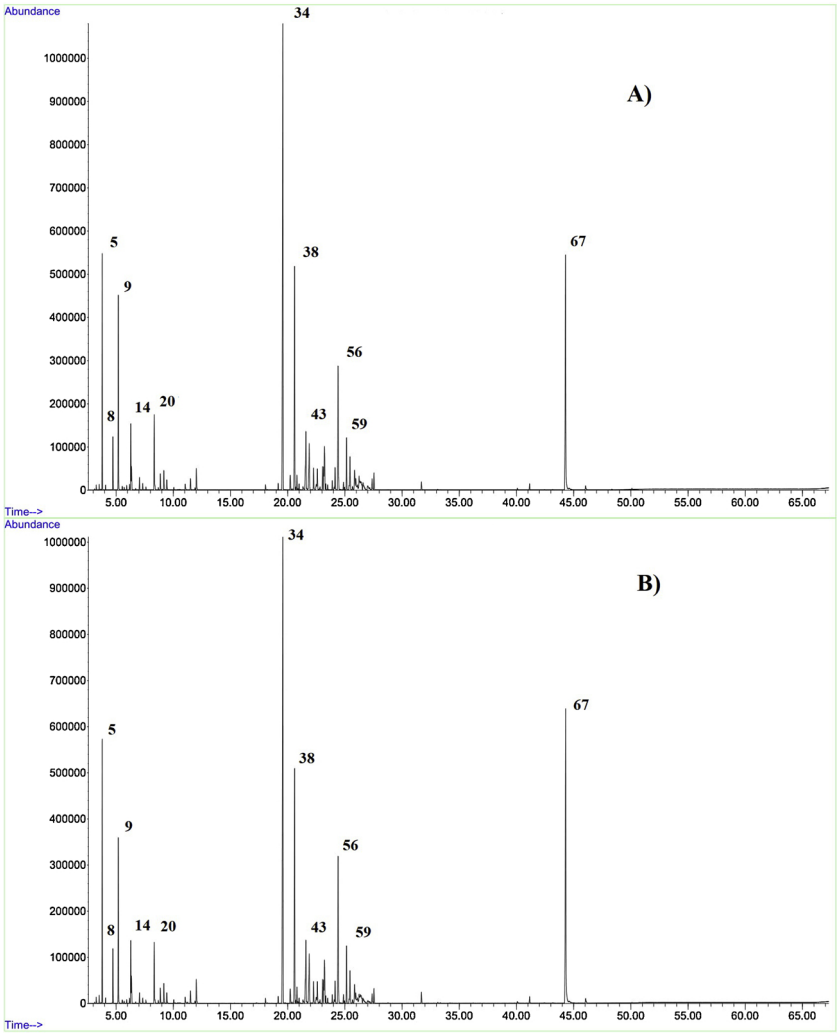

Fig. 7. GC–MS chromatograms of the hemp essential oil obtained by (A) HD and (B) MAE (V1 in Table 3). Peak numbering refers to Table 4.

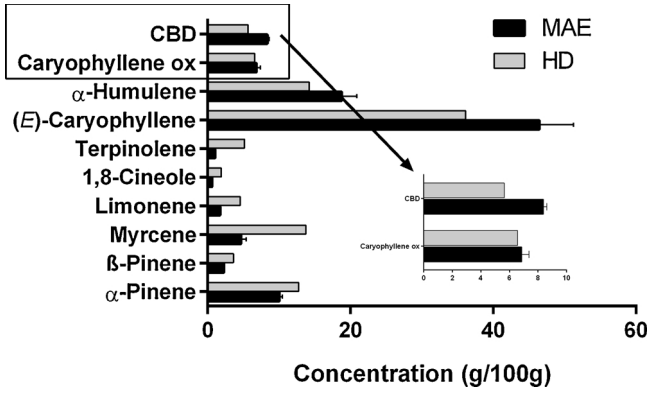

Fig. 8. Comparison between the marker bioactive compounds concentration in the hemp essential oil obtained by hydrodistillation (HD) and microwave-assisted extraction (MAE) (V1 in Table 3).

Table 5
Enantiomeric distribution of the major chiral components in the hemp essential oil obtained by MAE.

Enantiomer compund	RT [a]	RI [b]	MAE [f]		
			% in EO [c]	Enant. % [d]	ee% [e]
(-)-α-pinene	15.627	1022	0.33	4.92	
(+)-α-pinene	15.964	1028	6.44	95.08	90.17
(+)-β-pinene	19.24	1081	1.81	87.09	74.17
(-)-β-pinene	19.50	1085	0.27	12.91	
(+)-limonene	20.22	1097	2.48	93.25	86.50
(-)-limonene	20.52	1102	0.18	6.75	
(-)-(*E*)-caryophyllene	44.74	1497	35.57	100.00	100.00
(-)-caryophyllene oxide	57.44	1740	3.94	100.00	100.00

[a] The retention time of the different enantiomers from the chiral column (HP Chiral 20β) was as indicated in the table.
[b] Linear retention index calcuated using a mixture of *n*-alkanes (C_7-C_{30}).
[c] Absolute content of individual enantiomers in the oil; data from GC-FID analysis.
[d] Relative content of enantiomeric pairs.
[e] Enantiomeric excess.
[f] Data refer to run 8 included in Table 1.

CRediT authorship contribution statement

Dennis Fiorini: Formal analysis, Funding acquisition, Investigation, Writing - original draft, Writing - review & editing. **Serena Scortichini:** Formal analysis, Investigation, Methodology. **Giulia Bonacucina:** Writing - review & editing. **Nicolas G. Greco:** Formal analysis, Investigation, Methodology. **Eugenia Mazzara:** Formal analysis, Investigation, Methodology. **Riccardo Petrelli:** Funding acquisition, Writing - review & editing. **Jacopo Torresi:** Formal analysis, Investigation, Methodology. **Filippo Maggi:** Conceptualization,

Funding acquisition, Supervision, Writing - original draft, Writing - review & editing. **Marco Cespi:** Conceptualization, Data curation, Formal analysis, Investigation, Methodology, Software, Validation, Writing - original draft, Writing - review & editing.

Declaration of Competing Interest

Authors declare no competing interest.

Acknowledgements

The authors thank the Coop Canapa for providing the plant material, FKV – Milestone Srl for its assistance during the optimization procedure of ETHOS X, and Regione Marche (Programma di Sviluppo Rurale 2014/2020 – M16.1.A.2 Finanziamento dei Gruppi Operativi PSRMarche20142020_M16.1.A.2_ID_SIAR29012) and the University of Camerino (Fondo di Ateneo per la Ricerca) for financial support.

Appendix A. Supplementary data

Supplementary material related to this article can be found, in the online version, at doi:https://doi.org/10.1016/j.indcrop.2020.112688.

References

Abedi, A.-S., Rismanchi, M., Shahdoostkhany, M., Mohammadi, A., Mortazavian, A.M., 2017. Microwave-assisted extraction of *Nigella sativa* L. essential oil and evaluation of its antioxidant activity. J. Food Sci. Technol. 54, 3779–3790.

Adams, R., 2007. Identification of Essential Oil Components by Gas Chromatography/ Mass Spectrometry, 4th ed. Allured Publishing Corp., Carol Stream, IL, USA.

Amaducci, S., Zatta, A., Raffanini, M., Venturi, G., 2008. Characterisation of hemp (*Cannabis sativa* L.) roots under different growing conditions. Plant Soil 313, 227–235.

Appendino, G., Chianese, G., Taglialatela-Scafati, O., 2011. Cannabinoids: occurrence and medicinal chemistry. Curr. Med. Chem. 18, 1085–1099.

Barnes, M.P., 2006. Sativex®: clinical efficacy and tolerability in the treatment of symptoms of multiple sclerosis and neuropathic pain. Expert Opin. Pharmacother. 7, 607–615.

Benelli, G., Pavela, R., Lupidi, G., Nabissi, M., Petrelli, R., Kamte, S.L.N., Cappellacci, L., Fiorini, D., Sut, S., Dall'Acqua, Maggi, F., 2018a. The crop-residue of fiber hemp cv. Futura 75: from a waste product to a source of botanical insecticides. Environ. Sci. Pollut. Res. 25, 10515–10525.

Benelli, G., Pavela, R., Petrelli, R., Cappellacci, L., Santini, G., Fiorini, D., Sut, S., Dall'Acqua, S., Canale, A., Maggi, F., 2018b. The essential oil from industrial hemp (*Cannabis sativa* L.) by-products as an effective tool for insect pest management in organic crops. Ind. Crops Prod. 122, 308–315.

Benelli, G., Govindarajan, M., Rajeswary, M., Vaseeharan, B., Alyahya, S.A., Alharbi, N.S., kadaikunnan, S., Khaled, J.M., Maggi, F., 2018c. Insecticidal activity of camphene, zerumbone and α-humulene from *Cheilocostus speciosus* rhizome essential oil against the Old-World bollworm, *Helicoverpa armigera*. Ecotoxicol. Environ. Saf. 148, 781–786.

Bertoli, A., Tozzi, S., Pistelli, L., Angelini, L.G., 2010. Fiber hemp inflorescences: from crop-residues to essential oil production. Ind. Crops Prod. 32, 329–337.

Bordiga, M., Nollet, L.M., 2019. Food Aroma Evolution: During Food Processing, Cooking, and Aging. CRC Press.

Calzolari, D., Magagnini, G., Lucini, L., Grassi, G., Appendino, G.B., Amaducci, S., 2017. High added-value compounds from *Cannabis* threshing residues. Ind. Crops Prod. 108, 558–563.

Cappelletto, P., Brizzi, M., Mongardini, F., Barberi, B., Sannibale, M., Nenci, G., Poli, M., Corsi, G., Grassi, G., Pasini, P., 2001. Italy-grown hemp: yield, composition and cannabinoid content. Ind. Crops Prod. 13, 101–113.

Chatterjee, S., Simonoff, J.S., 2013. Model building. Handbook of Regression Analysis. John Wiley & Sons Inc., Hoboken, NewJersey (USA).

Chicca, A., Caprioglio, D., Minassi, A., Petrucci, V., Appendino, G., Taglialatela-Scafati, O., Gertsch, J., 2014. Functionalization of β-caryophyllene generates novel polypharmacology in the endocannabinoid system. ACS Chem. Biol. 9, 1499–1507.

Dahmane, D., Dob, T., Chelghoum, C., 2015. Chemical composition and analyses of enantiomers of essential oil obtained by steam distillation of *Juniperus oxycedrus* L. growing in Algeria. J. Mater. Environ. Sci. 6, 3159–3167.

Devinsky, O., Verducci, C., Thiele, E.A., Laux, L.C., Patel, A.D., Filloux, F., Szaflarski, J.P., Wilfong, A., Clark, G.D., Park, Y.D., Seltzer, L.E., Bebin, E.M., Flamini, R., Wechsler, R.T., Friedman, D., 2018. Open-label use of highly purified CBD (Epidiolex®) in patients with CDKL5 deficiency disorder and Aicardi, Dup15q, and Doose syndromes. Epilepsy Behav. 86, 131–137.

Di Candilo, M., 2006. Lo sviluppo della canapa tessile passa dalla raccolta meccanica. Informatore Agrario 62, 89.

Di Pierro, F., 2015. A nutraceutical role for cannabidiol. Why not? Nutrafoods 14, 111–117.

Do Vale, T.G., Furtado, E.C., Santos Jr, J.G., Viana, G.S.B., 2002. Central effects of citral, myrcene and limonene, constituents of essential oil chemotypes from *Lippia alba* (Mill.) NE Brown. Phytomedicine 9, 709–714.

FFNSC 3, 2015. Mass Spectra of Flavors and Fragrances of Natural and Synthetic Compounds, 3rd edition. John Wiley & Sons, Inc., Hoboken, NJ.

Fidyt, K., Fiedorowicz, A., Strządała, L., Szumny, A., 2016. β-caryophyllene and β-caryophyllene oxide - natural compounds of anticancer and analgesic properties. Cancer Med. 5, 3007–3017.

Filly, A., Fernandez, X., Minuti, M., Visinoni, F., Cravotto, G., Chemat, F., 2014. Solvent-free microwave extraction of essential oil from aromatic herbs: from laboratory to pilot and industrial scale. Food Chem. 150, 193–198.

Fine, P.G., Rosenfeld, M.J., 2013. The endocannabinoid system, cannabinoids, and pain. Rambam Maimonides Med. J. 4 (4).

Finnan, J., Styles, D., 2013. Hemp: a more sustainable annual energy crop for climate and energy policy. Energy Policy 58, 152–162.

Fiorini, D., Molle, A., Nabissi, M., Santini, G., Benelli, G., Maggi, F., 2019. Valorizing industrial hemp (*Cannabis sativa* L.) by-products: cannabidiol enrichment in the inflorescence essential oil optimizing sample pre-treatment prior to distillation. Ind. Crops Prod. 128, 581–589.

Forster, M.R., 2000. Key concepts in model selection: performance and generalizability. J. Math. Psychol. 52 (3), 345–370.

Gertsch, J., 2008. Anti-inflammatory cannabinoids in diet: towards a better understanding of CB(2) receptor action? Commun. Integr. Biol. 1, S26–S28.

Gertsch, J., 2018. Analytical and pharmacological challenges in Cannabis research. Planta Med. 84 213-213.

Hanušová, V., Caltová, K., Svobodová, H., Ambrož, M., Skarka, A., Murínová, N., Králova, V., Tomšik, P., Skálová, L., 2017. The effects of β-caryophyllene oxide and trans-nerolidol on the efficacy of doxorubicin in breast cancer cells and breast tumor-bearing mice. Biomed. Pharmacother. 95, 828–836.

Happyana, N., Agnolet, S., Muntendam, R., Van Dam, A., Schneider, B., Kayser, O., 2013. Analysis of cannabinoids in laser-microdissected trichomes of medicinal *Cannabis sativa* using LCMS and cryogenic NMR. Phytochemistry 87, 51–59.

Iseppi, R., Brighenti, V., Licata, M., Lambertini, A., Sabia, C., Messi, P., Pellati, F., Benvenuti, S., 2019. Chemical characterization and evaluation of the antibacterial activity of essential oils from fibre-type *Cannabis sativa* L. (Hemp). Molecules 24, 2302.

Jastrząb, A., Gęgotek, A., Skrzydlewska, E., 2019. Cannabidiol regulates the expression of keratinocyte proteins involved in the inflammation process through transcriptional regulation. Cells 8, 827.

Legault, J., Pichette, A., 2007. Potentiating effect of β-caryophyllene on anticancer activity of α-humulene, isocaryophyllene and paclitaxel. J. Pharm. Pharmacol. 59, 1643–1647.

Lewis, G.A., Mathie, D., Phan-Tan-Luu, R., 1999a. Response surface methodology. Pharmaceutical Experimental Design. Marcel Dekker, Inc., New York, USA.

Lewis, G.A., Mathieu, D., Phan-Tan-Luu, R., 1999b. Optimization. Pharmaceutical Experimental Design. Marcel Dekker, Inc., New York, USA.

Lewis, M.A., Russo, E.B., Smith, K.M., 2018. Pharmacological foundations of cannabis chemovars. Planta Med. 84, 225–233.

Lodzki, M., Godin, B., Rakou, L., Mechoulam, R., Gallily, R., Touitou, E., 2003. Cannabidiol—transdermal delivery and anti-inflammatory effect in a murine model. J. Control. Release 93, 377–387.

Lucchesi, M.E., Chemat, F., Smadja, J., 2004. Solvent-free microwave extraction of essential oil from aromatic herbs: comparison with conventional hydro-distillation. J. Chromatography A 1043, 323–327.

Mead, A., 2017. The legal status of cannabis (marijuana) and cannabidiol (CBD) under US law. Epilepsy Behav. 70, 288–291.

Milestone srl, 2019. Improving the Quality and Efficiency of Terpene Extraction from Cannabis plant: Application Report Ethos X - Terpenes.

Minitab 18 Support a, 2020. What Are Individual Desirability and Composite Desirability? https://support.minitab.com/en-us/minitab/18/help-and-how-to/modeling-statistics/using-fitted-models/supporting-topics/response-optimization/what-are-individual-desirability-and-composite-desirability/.

Minitab 18 Support b, 2020. Types of Confidence Intervals Used for Prediction. https://support.minitab.com/en-us/minitab/18/help-and-how-to/modeling-statistics/using-fitted-models/supporting-topics/prediction/confidence-intervals-for-prediction/.

Minitab blog, 2013. Multiple Regression Analysis: Use Adjusted R-Squared and Predicted R-Squared to Include the Correct Number of Variables. https://blog.minitab.com/blog/adventures-in-statistics-2/multiple-regession-analysis-use-adjusted-r-squared-and-predicted-r-squared-to-include-the-correct-number-of-variables.

Mollaei, S., Sedighi, F., Habibi, B., Hazrati, S., Asgharian, P., 2019. Extraction of essential oils of *Ferulago angulata* with microwave-assisted hydrodistillation. Ind. Crops Prod. 137, 43–51.

Morelli, M.B., Offidani, M., Alesiani, F., Discepoli, G., Liberati, S., Olivieri, A., Santoni, M., Santoni, G., Leoni, P., Nabissi, M., 2014. The effects of cannabidiol and its synergism with bortezomib in multiple myeloma cell lines. A role for transient receptor potential vanilloid type-2. Int. J. Cancer 134, 2534–2546.

Nabissi, M., Morelli, M.B., Offidani, M., Amantini, C., Gentili, S., Soriani, A., Cardinali, C., Leoni, P., Santoni, G., 2016. Cannabinoids synergize with carfilzomib, reducing multiple myeloma cells viability and migration. Oncotarget 7, 77543.

Nagy, D.U., Cianfaglione, K., Maggi, F., Sut, S., Dall'Acqua, S., 2019. Chemical characterization of leaves, male and female flowers from spontaneous Cannabis (*Cannabis sativa* L.) growing in Hungary. Chem. Biodivers. 16, e1800562.

Nahler, G., Jones, T.M., Russo, E.B., 2019. Cannabidiol and contributions of major hemp phytocompounds to the "Entourage Effect"; possible mechanisms. J. Altern. Complementary Integr. Med 5.

NIST 17, 2017. Mass Spectral Library (NIST/EPA/NIH). National Institute of Standards

and Technology, Gaithersburg, USA.
Palmieri, B., Laurino, C., Vadalà, M., 2019. Spontaneous, anecdotal, retrospective, open-label study on the efficacy, safety and tolerability of cannabis galenical preparation (Bedrocan). Int. J. Pharm. Pract. 27, 264–270.
Park, S.H., Staples, S.K., Gostin, E.L., Smith, J.P., Vigil, J.J., Seifried, D., Kinney, C., Pauli, C.S., Heuvel, B.D.V., 2019. Contrasting roles of cannabidiol as an insecticide and rescuing agent for ethanol–induced death in the tobacco hornworm *Manduca sexta*. Sci. Rep. 9, 1–10.
Pavela, R., Maggi, F., Lupidi, G., Cianfaglione, K., Dauvergne, X., Bruno, M., Benelli, G., 2017. Efficacy of sea fennel (*Crithmum maritimum* L., Apiaceae) essential oils against *Culex quinquefasciatus* say and *Spodoptera littoralis* (Boisd.). Ind. Crops Prod. 109, 603–610.
Pavela, R., Benelli, G., Canale, A., Maggi, F., Mártonfi, P., 2020. Exploring essential oils of Slovak medicinal plants for insecticidal activity: the case of *Thymus alternans* and *Teucrium montanum* subsp. *jailae*. Food Chem. Toxicol in press.
Petigny, L., Périno, S., Minuti, M., Visinoni, F., Wajsman, J., Chemat, F., 2014. Simultaneous microwave extraction and separation of volatile and non-volatile organic compounds of boldo leaves. From lab to industrial scale. Int. J. Mol. Sci. 15, 7183–7198.
Ranalli, P., Venturi, G., 2004. Hemp as a raw material for industrial applications. Euphytica 140, 1–6.
Regulation (EC), 2004. Regulation (EC) No 206/2004 of the European Parliament and of the Council amending Regulation (EC) No 2316/1999 laying down detailed rules for the application of Council Regulation (EC) No 1251/1999 establishing a support system for producers of certain arable crops. Offic. J. Eur. Commun. L34, 33.
Regulation (EC), 2007. Regulation (EC) No 834/2007 of 28 June 2007 on organic production and labelling of organic products and repealing Regulation (EEC) No 2092/91. Offic. J. Eur. Commun. L189, 20–27.
Russo, E.B., 2011. Taming THC: potential cannabis synergy and phytocannabinoid-terpenoid entourage effects. Br. J. Pharmacol. 163, 1344–1364.
Russo, E.B., 2016. Beyond cannabis: plants and the endocannabinoid system. Trends Pharmacol. Sci. 37, 594–605.
Scuderi, C., Filippis, D.D., Iuvone, T., Blasio, A., Steardo, A., Esposito, G., 2009. Cannabidiol in medicine: a review of its therapeutic potential in CNS disorders. Phytother. Res. 23, 597–602.
Silva, A.C.R.D., Lopes, P.M., Azevedo, M.M.B.D., Costa, D.C.M., Alviano, C.S., Alviano, D.S., 2012. Biological activities of a-pinene and β-pinene enantiomers. Molecules 17, 6305–6316.
Stahl, E., Kunde, R., 1973. Die Leitsubstanzen Der Haschisch- suchhunde. Kriminalistik: Z Gesamte Kriminal Wiss. Prax. 27, 385–389.
Sut, S., Maggi, F., Nicoletti, M., Baldan, V., Dall'Acqua, S.A., 2018. New drugs from old natural compounds: scarcely investigated sesquiterpenes as new possible therapeutic agents. Curr. Med. Chem. 25, 1241–1258.
Tabari, M.A., Khodashenas, A., Jafari, M., Petrelli, R., Cappellacci, L., Nabissi, M., Maggi, F., Pavela, R., Youssefi, M.R., 2020. Acaricidal properties of hemp (*Cannabis sativa* L.) essential oil against *Dermanyssus gallinae* and *Hyalomma dromedarii*. Ind. Crops Prod. 147, 112238.
Turk, M., Mathe, C., Fabiano-Tixier, A.S., Carnaroglio, D., Chemat, F., 2018. Parameter optimization in microwave-assisted distillation of frankincense essential oil. C. R. Chim. 21, 622–627.
Van den Dool, H., Kratz, P.D., 1963. A generalization of the retention index system including linear temperature programmed gas—liquid partition chromatography. J. Chromatogr. A 11, 463–471.
Veggi, P.C., Martinez, J., Meireles, M.A.A., 2012. Fundamentals of microwave extraction. In: Chemat, F., Cravotto, G. (Eds.), Microwave-Assisted Extraction for Bioactive Compounds. Food Engineering Series. Springer, Boston (USA), pp. 15–52.
Vukčević, M.M., Kalijadis, A.M., Vasiljević, T.M., Babić, B.M., Laušević, Z.V., Laušević, M.D., 2015. Production of activated carbon derived from waste hemp (*Cannabis sativa*) fibers and its performance in pesticide adsorption. Microporous Mesoporous Mater. 214, 156–165.
Watt, G., Karl, T., 2017. In vivo evidence for therapeutic properties of cannabidiol (CBD) for alzheimer's disease. Front. Pharmacol. 8, 20.
Zuccaro, C., 1992. Mallows' cp statistic and model selection in multiple linear regression. Int. J. Sales Mark. Manag. Res. Dev. 34.